HHS Public Access

Author manuscript

Sci Signal. Author manuscript; available in PMC 2022 September 02.

Published in final edited form as:

Sci Signal. ; 10(491): . doi:10.1126/scisignal.aal2880.

The tyrosine phosphatase SHP-1 promotes T cell adhesion by activating the adaptor protein CrkII in the immunological synapse

Inbar Azoulay-Alfaguter[1], **Marianne Strazza**[1], **Michael Peled**[1], **Hila K. Novak**[2,3], **James Muller**[2], **Michael L. Dustin**[2,3], **Adam Mor**[1,2,4,*]

[1]Department of Medicine, New York University School of Medicine, New York, NY 10016, USA.

[2]Department of Pathology, New York University School of Medicine, New York, NY 10016, USA.

[3]Kennedy Institute for Rheumatology, Oxford University, Oxford, UK.

[4]Perlmutter Cancer Center, New York University School of Medicine, New York, NY 10016, USA.

Abstract

The adaptor protein CrkII regulates T cell adhesion by recruiting the guanine nucleotide exchange factor C3G, an activator of Rap1. Subsequently, Rap1 stimulates the integrin LFA-1, which leads to T cell adhesion and interaction with antigen-presenting cells (APCs). The adhesion of T cells to APCs is critical for their proper function and education. The interface between the T cell and the APC is known as the immunological synapse. It is characterized by the specific organization of proteins that can be divided into central supramolecular activation clusters (c-SMACs) and peripheral SMACs (p-SMACs). Through total internal reflection fluorescence (TIRF) microscopy and experiments with supported lipid bilayers, we determined that activated Rap1 was recruited to the immunological synapse and localized to the p-SMAC. C3G and the active (dephosphorylated) form of CrkII also localized to the same compartment. In contrast, inactive (phosphorylated) CrkII was confined to the c-SMAC. Activation of CrkII and its subsequent movement from the c-SMAC to the p-SMAC depended on the phosphatase SHP-1, which acted downstream of the T cell receptor. In the p-SMAC, CrkII recruited C3G, which led to Rap1 activation and LFA-1–mediated adhesion of T cells to APCs. Functionally, SHP-1 was necessary for both the adhesion and migration of T cells. Together, these data highlight a signaling pathway in which SHP-1 acts through CrkII to reshape the pattern of Rap1 activation in the immunological synapse.

INTRODUCTION

T lymphocytes are central to the adaptive immune response in both beneficial and harmful settings (1, 2). Adhesion is an essential aspect of T cell biology; without proper adhesion,

*Corresponding author. adam.mor@nyumc.org.

Author contributions:

I.A.-A. and A.M. planned the experiments. I.A.-A. and A.M. performed the experiments. I.A.-A., M.S., and M.P. analyzed the data and provided comments. H.K.N. and J.M. supported the SLB experiments. M.L.D. contributed to the design and interpretation of the SLB experiments. I.A.-A. and A.M. wrote the manuscript.

Competing interests:

The authors declare that they have no competing interests.

T cells can neither traffic to appropriate compartments nor recognize antigens presented on major histocompatibility complexes (3). Effective T cell adhesion is also essential for autoimmunity, suggesting that adhesive function may be a target for treating diseases such as rheumatoid arthritis, lupus, and psoriasis (3). However, the potential for therapeutically ameliorating autoimmune conditions by modulating T cell adhesion has thus far been limited by adverse events (3). To identify more selective adhesion control points, it is imperative to better understand the molecular mechanisms regulating T cell adhesion (4–6).

The integrin LFA-1 is a critical adhesion molecule for T cell interactions with antigen-presenting cells (APCs) (7). The affinity of LFA-1 for its ligand intercellular adhesion molecule–1 (ICAM-1) varies with activation state and is determined by the small guanosine triphosphatase (GTPase) Ras-related protein 1 (Rap1) (8) and the organization of the actin cytoskeleton (9). The ability of Rap1 to control the affinity of LFA-1 for ICAM-1, and thus T cell adhesion, is well established, although the pathway connecting the T cell receptor (TCR) and Rap1 is incompletely elucidated (10). The adaptor protein CrkII (chicken tumor virus regulator of kinase II) is a key regulator of T cell adhesion through the recruitment of a Rap1 guanine nucleotide exchange factor (GEF), C3G [Crk SH3 (Src homology 3) domain binding guanine nucleotide–releasing factor]. How CrkII is phosphorylated downstream of the TCR and the subcellular localization of C3G in the immunological synapse are not clear.

The physiological relevance of Rap1 is evident in patients suffering from a congenital defect in Kindlin-3, which is required for proper Rap1 signaling (11, 12). Such patients manifest leukocyte adhesion deficiency type III syndrome, an immunodeficiency and blood clotting disorder (13). Rap1 cycles between active [guanosine triphosphate (GTP)–bound] and inactive [guanosine diphosphate (GDP)–bound] conformations (8, 14). As for all small GTPases, Rap1 activation is regulated by GEFs that cause Rap1 to release GDP in favor of GTP and by GTPase-activating proteins (GAP) that enhance the slow intrinsic GTPase reaction (8, 15). One important Rap1 GEF, C3G, is highly abundant in T lymphocytes (16, 17). The C terminus of C3G consists of the CDC25 homology domain, which is the catalytic domain of members of the Ras family. The N-terminal region of C3G inhibits its GEF activity. Secondary to TCR signaling, C3G translocates from the cytosol to the plasma membrane (18) and becomes phosphorylated on Tyr^{504} (16), and then, the inhibition mediated by its N-terminal region is repressed to increase GEF activity.

The adaptor protein CrkII is essential for C3G function (16). CrkII is involved in the early steps of lymphocyte activation through its SH2-mediated interaction with TCR-proximal signaling proteins, such as Casitas B-lineage lymphoma proto-oncogene (Cbl), ζ chain of TCR-associated protein kinase 70 (Zap70), Crk-associated substrate-related protein (CasL), and signal transducer and activator of transcription 5 (STAT5) (19). In addition, CrkII constitutively associates through its SH3 domain with C3G. Studies demonstrated that the conformation and function of CrkII are subjected to regulation by immunophilins (20), which also affect CrkII-dependent T cell adhesion and migration (21). Through experiments with conditional knockout mice, Huang *et al.* reported that T cells lacking CrkII exhibit reduced integrin-mediated adhesion and chemotaxis (22). The authors also determined that CrkII coordinated C3G to activate Rap1 (22). This study established a role for CrkII in the selective regulation of T cell adhesion and migration at effector sites in response to

chemokines; however, it did not address directly the role of C3G as the GEF downstream of the TCR.

The immunological synapse describes stable, antigen-specific adhesive junctions formed between T cells and APCs, which may include well-organized supramolecular activation clusters (SMACs) (23). SMACs comprise concentric rings that contain segregated clusters of proteins driven by TCR signaling. The central SMAC (c-SMAC) is enriched in costimulatory receptors, such as CD28; the peripheral SMAC (p-SMAC) is enriched in LFA-1–ICAM-1 interactions; and the distal SMAC (d-SMAC) is enriched in F-actin and the transmembrane phosphatase CD45 (24). These structures are found at the interface between two cells (such as an APC and a T cell) and can be modeled with a supported lipid bilayer (SLB) that contains proteins that diffuse within the bilayer to mimic the membrane of the APC. Total internal reflection fluorescence (TIRF) microscopy is ideal for high-contrast imaging of fluorescently tagged molecules involved in immunological synapse formation in the SLB system. In experiments with single activated T cells, our group and others have reported that the activated pool of Rap1 decorates both the plasma membrane and the vesicular compartments (18, 25, 26). However, the distribution of Rap1 within different compartments of the immunological synapse, its interaction with TCR-proximal signaling components in this setting, and its functions and contribution to productive synapses are unknown.

The main aim of this work was to uncover the biology of Rap1 in the immunological synapse. Using TIRF microscopy, we discovered that both Rap1 and the exchange factor C3G were localized to the p-SMAC. Moreover, we showed that dephosphorylation of the adaptor protein CrkII downstream of stimulation of the TCR was required for C3G activity and subsequent Rap1 activation. Furthermore, dephosphorylation of CrkII was mediated by the phosphatase SHP-1 and contributed to multiple T cell functions, including adhesion, migration, and cytokine secretion.

RESULTS

Activated Rap1 is recruited to the immunological synapse

We and others (8) showed that stimulation of the TCR with an anti-CD3 antibody resulted in the activation of Rap1 at the plasma membrane (14, 25–27). One of the main characteristics of immunological synapse formation is polarization and recruitment of TCR-proximal signaling proteins toward the contact area. A study by Cote *et al.* documented the recruitment of Rap1 to the immunological synapse in fixed cells, but whether this pool of Rap1 is activated (GTP-bound) is not clear (26). To find out where in the cell Rap1 is activated during immunological synapse formation, we used Jurkat cells expressing green fluorescent protein (GFP)–tagged RalGDS-RBD [Ras-binding domain (RBD) of the protein Ral guanine nucleotide dissociation stimulator (RalGDS); a probe for activated Rap1] cocultured with Raji cells (a B cell line that acts as APCs) preloaded with *Staphylococcus* enterotoxin E (SEE). Rap1 activation in live cells was limited to the contact area between the cells in 82% of the stable conjugates (Fig. 1A, bottom). Polarized Rap1 recruitment was specific to cells stimulated through the TCR because Rap1 was recruited to the contact area

in the absence of SEE in only 16% of cells that formed stable conjugates (Fig. 1A, top, and fig. S1).

Because antibody-mediated stimulation of cells has limited physiological relevance, we confirmed the recruitment of GTP-loaded Rap1 to the immunological synapse in experiments in which we activated T cells with natural ligands found on APCs. Specifically, we cocultured OT-II T cells (26) expressing GFP-RalGDS-RBD with dendritic cells (DCs) loaded with ovalbumin (OVA) peptide. Activated Rap1 was enriched in the contact area of 65% of the cells stimulated through the TCR (Fig. 1B), suggesting that Rap1 activation occurs at the immunological synapse of primary murine T cells.

To resolve the distribution of Rap1 in the immunological synapse, we used the SLB model and TIRF microscopy (fig. S2). When primary human T cells were added to a bilayer containing anti-CD3 antibody and recombinant ICAM-1, Rap1 was excluded from the c-SMAC in synapse at both early (5 min) and late (20 min) times (Fig. 1, C and D). To show that this exclusion was not secondary to physical retraction, we used a modified version of GFP (GFP-CAAX) that was tethered to the plasma membrane and showed that it was present in both the c-SMAC and the p-SMAC (fig. S3). The closely related GTPase Ras (17) was not excluded from the c-SMAC (Fig. 1, C and D). Furthermore, whereas the pool of activated (GTP-loaded) Rap1 was also excluded from the c-SMAC, GTP-loaded Ras showed marked accumulation in the c-SMAC (Fig. 1, C and E). Thus, activated Rap1 appeared to be polarized to the cell-cell contact area during synapse formation.

The factors regulating Rap1 localization in the immunological synapse are analyzed

The ability of Rap1 to interact with lipid membranes is by virtue of the attachment of a geranylgeranyl lipid to its hypervariable region as well as by the affinity of its adjacent positively charged sequence to the inner leaflet of the plasma membrane (28–30). When we expressed a variant of Rap1 in which the 20-carbon geranylgeranyl lipid tail was replaced by the 15-carbon prenyl group of Ras (by changing the CAAX domain in the hypervariable region into CVVM) (fig. S4), Rap1 lost its distinct distribution and was no longer excluded from the c-SMAC (Fig. 2, A and B), suggesting that the 20-carbon, but not the 15-carbon, tail of Rap1 was required for its compartmentalization within the immunological synapse.

Previously, we showed that Rap1 is localized to the plasma membrane (18). Here, in experiments with the RalGDS-RBD probe, we demonstrated that this pool of Rap1 was GTP-loaded (Fig. 1). To identify whether the activation status of Rap1 contributed to its localization in the immunological synapse, we overexpressed activated ($Rap1^{G12V}$) and inactivated ($Rap1^{S17N}$) variants of Rap1 in primary human T cells. We found that, despite the variants being present in similar amounts (fig. S5), the activated pool of Rap1 was excluded from the c-SMAC, whereas the inactivated pool of Rap1 failed to decorate any part of the immunological synapse (Fig. 2, A and C). This finding suggests that despite the presence of a plasma membrane pool of inactivated Rap1 (GFP-Rap1 and GFP-RalGDS-RBD did not share the same subcellular distribution in activated cells), the pool of Rap1 in the immunological synapse is exclusively GTP-loaded.

It is appreciated that the subcellular localization of multiple small GTPases is determined by the distribution of their specific GEFs and GAPs (15, 31). We found that the major GEF for Rap1 in T cells, C3G [either wild-type C3G or the activated variant ($C3G^{Y504D}$)], was also excluded from the c-SMAC (Fig. 2, A and D). This property was particular to C3G because another Rap1 GEF, CalDAG-GEFIII (15, 32), failed to show a similar distribution (Fig. 2, A and D). Whereas it is not surprising that C3G was localized to the immunological synapse, why it (unlike other GEFs) was excluded from the c-SMAC is unclear. Thus, multiple processes, such as lipidation, activation, and the presence of specific GEFs, contribute together to ensure the appropriate localization of Rap1 in the immunological synapse.

CrkII phosphorylation is required for its proper localization in the immunological synapse

CrkII is anadaptor protein that binds to several tyrosine-phosphorylated proteins and is required for proper localization of the GEF C3G (20, 21, 33, 34). Nath *et al.* found that binding between these proteins and subsequent T cell adhesions were dependent on the peptidyl–prolyl isomerase immunophilins (20). We validated the ability of dephosphorylated CrkII to interact with C3G (fig. S6, A and B). Upon phosphorylation, CrkII folds on itself to cover its SH2- and SH3-binding sites and thus becomes inactive (Fig. 3A) (21, 35). Whereas the phosphodeficient (active) variant of CrkII ($CrkII^{Y221A}$) was found at the same location as C3G (Figs. 2A and 3B) and Rap1 (Fig. 2C), the phosphomimetic (inactive) variant of CrkII ($CrkII^{Y221D}$) was restricted to the c-SMAC in primary human T cells (Fig. 3, B and C). To further support this finding and to validate that wild-type CrkII translocated between different compartments of the immunological synapse in a manner dependent on its phosphorylation state, we treated cells expressing CrkII with pervanadate, a tyrosine phosphatase inhibitor (36), and analyzed the distribution of CrkII (Fig. 3D). Despite the treatment with pervanadate leading to the phosphorylation of multiple proteins, we used a specific antibody to confirm that CrkII was among them and that its phosphorylation occurred at position 221 (fig. S7, A and B). We found that within 10 min of treating the cells with pervanadate, CrkII redeployed from the p-SMAC to the c-SMAC in most of the cells, presumably after it became phosphorylated at position 221 (Fig. 3, D and E). Together, these data suggest that dephosphorylated CrkII travels to the periphery of the immunological synapse, where it likely acts on its effector, C3G.

CrkII dephosphorylation leads to T cell activation

An important aim in our search to identify signaling molecules upstream of CrkII was to uncover the mechanism by which CrkII is dephosphorylated before its relocation to the p-SMAC. Given that CrkII is also a cytosolic protein, we first demonstrated that there was an increase in the amount of CrkII in the plasma membrane fraction upon TCR stimulation (fig. S8, A and B). The same treatment also resulted in a reduction in the amount of phosphorylated CrkII at two different times (Fig. 4, A and B). To validate this finding using an additional imaging approach, we expressed the PICCHUx vector [yellow fluorescent protein (YFP)–CrkII–cyan fluorescent protein (CFP)–CAAX] in T cells treated with anti-CD3 antibody (20). This fluorescence resonance energy transfer (FRET)–based construct was designed to report the folding status of CrkII (37). We detected a reduction in FRET efficiency upon stimulation of transiently transfected Jurkat cells through the TCR (Fig. 4, C and D), suggesting that engagement of the TCR resulted in the dephosphorylation of CrkII.

To show that CrkII dephosphorylation was associated with increased adhesion, we expressed phosphodeficient or phosphomimetic variants of CrkII in T cells and demonstrated that only the former resulted in an increased amount of GTP-Rap1 and the increased adhesion of the cells to ICAM-1–coated surfaces (Fig. 4, E and F). To confirm that CrkII^{Y221D} was folded properly, we expressed phosphomimetic and phosphodeficient variants of the PICCHUx construct (YFP-CrkII^{Y221D}-CFP-CAAX and YFP-CrkII^{Y221A}-CFP-CAAX, respectively) in Jurkat cells and detected high FRET efficiency in cells expressing the latter construct (fig. S9, A to C). To demonstrate the contribution of phosphodeficient (active) CrkII to cellular functions, we expressed CrkII^{Y221A} in T cells and stimulated them with anti-CD3 antibody in wells coated with ICAM-1 (to mimic the immunological synapse environment) (38) and found that they had an increase in the amount of the cell surface activation marker CD69 (Fig. 4G). CrkII^{Y221A} also enhanced the amount of interleukin-2 (IL-2) secreted by the cells stimulated in the same manner (Fig. 4H) (8, 39, 40). These findings suggest that stimulation of the TCR leads to the dephosphorylation of CrkII, which is associated with increased adhesion to ICAM-1, cellular activation, and IL-2 secretion.

SHP-1 dephosphorylates CrkII in response to TCR stimulation

To uncover the signaling events between stimulation of the TCR and CrkII dephosphorylation, we treated Jurkat cells with two phosphatase inhibitors, the nonspecific SHP-1/2 inhibitor NSC-87877 (41) and the PP2 inhibitor cantharidic acid (5, 42), and then measured the amount of phosphorylated CrkII in the cells upon treatment with anti-CD3 antibody. We found that only treatment with NSC-87877 resulted in the generation of increased amounts of phosphorylated CrkII (Fig. 5A). The same treatment also resulted in the reduced adhesion of anti-CD3 antibody–treated cells to ICAM-1–coated wells (Fig. 5B). This inhibition was blocked by overexpressing a phosphodeficient CrkII variant (CrkII^{Y221A}), which suggests that at least one of the targets for SHP-1 or SHP-2 is the adaptor protein CrkII (Fig. 5B). There are two main isoforms of the tyrosine phosphatase SHP: SHP-1 (*PTPN6*) and SHP-2 (*PTPN11*) (43). Both phosphatases are present in most tissues and play regulatory roles in various cell signaling events that are important for a diversity of cell functions, such as mitogenic activation, metabolic control, and cell migration (44). We knocked down each isoform individually (Fig. 5C and fig. S10) and then measured the abundance of phosphorylated CrkII. Whereas the amount of phosphorylated CrkII was unchanged, or decreased, in wild-type cells (scramble), upon knockdown of SHP-1 or SHP-2, there was a marked increase in CrkII phosphorylation after TCR stimulation (Fig. 5, D and E). Disruption of tonic CrkII phosphorylation, as governed by additional kinases and their corresponding positive and negative feedback loops, might also have contributed to CrkII function. The extent of the increase in CrkII phosphorylation was more substantial when SHP-1 was knocked down (Fig. 5E). Moreover, knocking down *SHP-1* inhibited TCR-stimulated static adhesion (45) to ICAM-1 in Jurkat cells expressing the relevant short hairpin RNA (shRNA) (Fig. 5F) and primary human T cells treated with small interfering RNA (siRNA) (Fig. 5G).

To confirm that the contribution of SHP-1 to adhesion was not compensated for by SHP-2 signaling, we knocked down SHP-1 alone or together with SHP-2 and found that adhesion to ICAM-1 was reduced to the same extent (Fig. 5G). To rule out off-target effects of our

inhibitory RNAs, we rescued the adhesion defect of the cells by overexpressing SHP-1 (Fig. 5H). Moreover, the phosphodeficient CrkII variant ($CrkII^{Y221A}$) also rescued this adhesion defect, suggesting that T cell adhesion is mediated specifically through CrkII dephosphorylation by SHP-1 (Fig. 5H). The contribution of SHP-1 to TCR signaling was also demonstrated by a chemokinesis assay (46), which showed that primary human T cells deficient in SHP-1 failed to arrest in response to TCR cross-linking (Fig. 5I). Using conjugate formation assays, we demonstrated that SHP-1 was required for the activation and recruitment of Rap1 to the contact area of Jurkat cells (Fig. 5J) and primary human T cells cocultured with APCs (Fig. 5K). Moreover, SHP-1 was also required for stable conjugate formation (Fig. 5L). Together, our results suggest that CrkII is targeted by SHP-1 upon TCR stimulation and that SHP-1 is required for Rap1 activation and T cell adhesion downstream of the TCR.

DISCUSSION

Previous work showed that the activation of Rap1 in response to TCR stimulation is mediated primarily by the exchange factor C3G (40, 47). C3G was the first Rap1 GEF identified, and it is highly abundant in T lymphocytes. C3G transduces signals from Crk proteins, binding to their SH3 domains and activating mainly Rap1 (and, to a lesser extent, other members of the Ras family of GTPases). The recruitment of C3G to the plasma membrane is facilitated by several adaptor proteins, including CrkII, CrkL, and CasL (48, 49). Unlike C3G, which is restricted to the p-SMAC, CrkII translocates from the p-SMAC to the c-SMAC upon phosphorylation (Fig. 6).

Compartmentalization of signaling molecules to different areas of the immunological synapse based on their phosphorylation state has been reported previously. Campi *et al.* reported that phosphorylated TCR clusters move to the c-SMAC (50), and Purbhoo *et al.* discovered that phosphorylated LAT clusters and vesicles move centripetally toward the c-SMAC during immunological synapse formation (51, 52). Analogously, we showed here that the phosphorylation state of CrkII was directly linked to its compartmentalization within the immunological synapse. However, the direction of its trafficking was not toward but rather away from the center of the synapse. Moreover, the localization of CrkII is also associated with multiple T cell functions, including adhesion and cytokine secretion. This is an example of how the subcellular localization of an adaptor protein can regulate downstream signaling (51, 53).

An additional level of CrkII regulation was demonstrated by previous studies showing an important role for its proline-rich domain and its ability to alter CrkII from a cis (inactive) to a trans (active) conformation (54, 55). In this regard, the previous studies showed that the binding of CrkII to C3G was enhanced by the activity of prolyl isomerases (20, 56, 57). The contribution of CrkII isomerization to its localization at different compartments of the immunological synapse is not clear.

The mechanism underlying the retention of dephosphorylated CrkII at the p-SMAC remains unclear. Previous reports showed that the adaptor protein CasL is limited to the same compartment (49, 58). We confirmed that CrkII and CasL physically interact with each other

(fig. S11, A and B), which suggests that CasL might serve as a docking site to retain CrkII in the periphery of the synapse, where it can signal downstream to Rap1 and LFA-1 (Fig. 6). In contrast to CrkII, the TCR complex travels to the center of the immunological synapse upon stimulation and during the maturation process. Whereas CrkII trafficking is regulated by dephosphorylation and possibly by its binding to CasL, the contribution of Rap1 and Ras signaling to TCR trafficking remains incompletely understood. Choudhuri *et al.* reported that polarized vesicles enriched in TCR complexes emerge from the center of the immunological synapse (59). Whether these vesicles are also enriched with activated Rap1 or Ras proteins is under active investigation in our laboratory.

Tyrosine phosphorylation (and dephosphorylation) of proteins plays a critical role in many T cell functions (43). The opposing actions of kinases and phosphatases determine the extent of tyrosine phosphorylation at any given time (60, 61). It is well appreciated that kinases are essential during T cell signaling to promote adhesion. Nolz *et al.* demonstrated that although the kinase Abl does not regulate the recruitment of C3G to the immunological synapse, it affects the phosphorylation of C3G itself, which is required for its GEF activity toward Rap1 (40). The role and importance of phosphatases to T cell functions are less well appreciated (43). Specifically, the roles of the phosphatases SHP-1 and SHP-2 in T cells are not clear because of numerous opposing reports showing that SHP-2 activity is related to activating pathways (62), whereas SHP-1 is associated with the inhibition of selected T cell functions (43). Analogous to the mechanism by which the phosphatase CD45 activates Lck, our data suggest that SHP-1 targets CrkII upon TCR stimulation, leading to the recruitment of C3G to the plasma membrane and the Rap1-dependent activation of LFA-1 at the immunological synapse (Fig. 6). Thus, our study reveals a previously uncharacterized function for SHP-1 in integrin-mediated adhesion downstream of TCR stimulation.

Despite the high degree of homology between Ras and Rap1, their localization in the immunological synapse was very different. Whereas activated Ras was limited to the c-SMAC, GTP-loaded Rap1 was excluded from the same compartment. We hypothesize that this is secondary to the differences in the sequences of the hypervariable regions of these GTPases, leading to diverse posttranslational modifications that ultimately support affinity for either the p-SMAC or the c-SMAC. Ongoing experiments in our laboratory will clarify these findings.

An observation that was not addressed in this work is the distinct pattern of distribution of CrkII and C3G. Both proteins exhibited a tightly clustered organization (Figs. 2A and 3B) within the immunological synapse. These clusters resemble talin microclusters (63), suggesting a possible interaction with the actin cytoskeleton (9, 64) or with other actin regulatory proteins, such as Wiskott-Aldrich syndrome protein (WASP) (65, 66), Src kinase–associated phosphoprotein (SKAP) (67, 68), regulator for cell adhesion and polarization enriched in lymphoid tissue (RapL) (14), Rap1-interacting adaptor molecule (RIAM) (15, 69), or Wiskott-Aldrich syndrome protein family member 2 (WASF2) (40). The role of the actin cytoskeleton and these proteins in the dynamics of CrkII trafficking will be a subject for future studies. Specifically, it was reported that the protein SLAT is crucial for the TCR-induced activation of LFA-1 and T cell adhesion (26). SLAT interacts, through its PH domain, with activated Rap1. This interaction facilitates the recruitment of Rap1 and

SLAT to the immunological synapse (26). Thus, the distribution of SLAT within different compartments of the synapse is of interest.

Together, our data show a previously uncharacterized regulatory pathway leading to T cell adhesion. TCR activation induced the dephosphorylation of plasma membrane–bound CrkII by SHP-1. The dephosphorylated CrkII protein translocated to the p-SMAC, where it interacted with C3G, which activated Rap1. Thus, we position CrkII and SHP-1 as critical players in immunological synapse formation and suggest that CrkII phosphorylation might be therapeutically manipulated to treat inflammatory diseases.

MATERIALS AND METHODS

General reagents

RPMI 1640 and Opti-MEM I were purchased from Invitrogen. Poly-L-lysine was purchased from Sigma. SEE was purchased from Toxin Technology. The BCA Protein Assay Kit was purchased from Pierce Biotechnology. Pervanadate was prepared by mixing orthovanadate (Sigma) and H_2O_2 (Sigma) at a 1:1 ratio and was used at a final concentration of 50 μM. NSC-87877 was purchased from Millipore. Cantharidic acid was obtained from Santa Cruz Biotechnology.

Cell culture, transfection, and stimulation

Jurkat and Raji cells were obtained from the American Type Culture Collection (ATCC). Cells were maintained in 5% CO_2 at 37°C in RPMI 1640 supplemented with 10% fetal bovine serum (FBS) and 1% penicillin/streptomycin. 293T cells were obtained from the ATCC and maintained in 5% CO_2 at 37°C in Dulbecco's modified Eagle's medium supplemented with 10% FBS and 1% penicillin/streptomycin. Human peripheral $CD3^+$ T lymphocytes were isolated by negative selection from whole blood with the RosetteSep Human CD3 T Cell Isolation Kit (STEMCELL Technologies), followed by separation over density gradient medium (Lymphoprep, STEMCELL Technologies). Primary cells were maintained in enriched medium containing 1% L-glutamine, 1% nonessential amino acids, 1% sodium pyruvate, and 1% Hepes at 5% CO_2 and 37°C. Plasmids were introduced into Jurkat cells, primary human cells, and primary mouse T cells by nucleofection (Lonza); a transfection efficiency of 50 to 70% was achieved in all experiments. Immobilized or soluble anti-CD3 antibody (1 to 5 mg/ml) and ICAM-1 (250 molecules/mm^2) were used for stimulation. Plasmids were introduced into 293T cells by SuperFect transfection reagent (Qiagen) according to the manufacturer's protocol.

Antibodies and recombinant proteins

Antibodies used in this study were as follows: anti-CD3 (BioLegend), anti-CD3 and anti-CD28 (Ancell), anti-pCrkII (Tyr^{221}; Cell Signaling), anti-CrkII (Santa Cruz Biotechnology), anti-RhoGDI (BD Biosciences), anti-C3G (Bethyl Laboratories), anti–SHP-1 (SH-PTP1)/SHP-2 (SH-PTP2) (Santa Cruz Biotechnology), anti-phosphotyrosine (4G10, Millipore), anti-Rap1 (Millipore), anti-GFP mAb-Agarose (MBL), anti-GFP (Invitrogen), anti-hemagglutinin (HA) (Abcam), and anti-CD69 phycoerythrin (PE) (eBioscience). Monobiotinylated anti-CD3 and Alexa Fluor 568 (Invitrogen)–conjugated

anti-CD3ε Fab′ (UCHT1) and ICAM-1–His12 AF 405 were generated as previously described (59). In solid-phase stimulation experiments, recombinant human ICAM-1–Fc (R&D Systems) was used.

Plasmids

Plasmid encoding GFP-C3G was a gift from P. Stork (Vollum Institute). Plasmids encoding Cherry-Rap1, GFP-RBD-RalGDS, GFP-Rap1, GFP–N-Ras, GFP-Raf1-RBD, GFP-Rap1^{G12V}, GFP-Rap1^{S17N}, GFP-C3G^{Y504V}, and CalDAGGEFIII were previously described (18, 25, 70, 71). Plasmid encoding GFP-CrkII was provided by K. Yamada (Addgene). The complementary DNAs (cDNAs) encoding GFP-Rap1-CVVL, CrkII^{Y221A}, and CrkII^{Y221D} were subcloned from pEGFPC1-Rap1 and pGFP-CrkII by an overlapping polymerase chain reaction (GFP-Rap1-CVVL, 5′-CCTAAAAAGAAATCATGTGTGGTGATGTAGGAATTCTGCAGTCGA-3′; CrkII^{Y221A}, 5′-CCGGAGCCTGGGCCCGCTGCCCAACCCAGCGTC-3′; CrkII^{Y221D}, 5′-CCGGAGCCTGGGCCCGATGCCCAACCCAGCGTC-3′). PICCHUx was a gift from M. Matsuda (Osaka University). The Flag-CasL-HA plasmid was provided by L. Chin (Addgene). The SHP-1–MSCV–IRES–GFP plasmid was a gift from B. Neel (New York University). Plasmids were treated with an UltraClean Endotoxin Removal kit (MO BIO Laboratories) and verified by bidirectional sequencing.

Conjugate formation assay

SEE-loaded Raji cells (1.5×10^6) were mixed with Jurkat cells (1.5×10^6), plated on 35-mm glass-bottom culture plates (ibidi GmbH) coated with poly-L-lysine (10 μg/ml), and subjected to brief centrifugation before being imaged. Images were taken with a Zeiss 700 confocal microscope and quantified for cell-cell conjugate formation, as previously described (fig. S2) (5, 6). OT-II T cells expressing a transgenic TCR that recognizes OVA were isolated from single-cell suspensions from the spleens of DO11.10 mice by depletion of magnetically labeled non-CD3 cells (Invitrogen). To isolate APCs, spleen suspensions were prepared by digestion with collagenase D (100 U/ml) in Hanks' balanced salt solution for 40 min. Low-density cells were isolated by centrifugation over a 60% Percoll gradient. Cells were further enriched by differential adherence by incubating the cells on 100-mm tissue culture plates in medium containing 5% FBS for 2 hours with OVA peptide (100 μg/ml).

Lipid bilayer experiments

Lipid bilayers were prepared as previously described (72). Liposomes containing biotin-CAP-phosphatidylethanolamine, phosphatidylcholine, and Ni^{2+}-chelating lipids (Avanti Polar Lipids) were placed on 40-mm glass coverslips cleaned with Piranha solution (Cyantek Corporation) to form the planar bilayers. After being blocked for 30 min with 5% casein, 100 μM $NiCl_2$, fluorescently labeled His–ICAM-1 (250 molecules/mm^2), and monobiotinylated Fab′ fragments of human anti-CD3ε antibodies (5 μg/ml), flow chambers were warmed up to 37°C and cells transfected with the relevant plasmids were injected in 200 μl of Hepes-buffered saline containing 1% human serum albumin (Sigma). Images were collected at different time points. For immunostaining, cells were fixed with 2% paraformaldehyde at room temperature for 20 min and then were permeabilized for 1 min

with 0.1% Triton X-100. The cells were then blocked with 5% casein for 30 min, washed, and then incubated with primary antibodies for 30 min and then with the appropriate secondary antibodies for an additional 20 min.

Microscopy

TIRF microscopy imaging was performed on a custom automated Nikon inverted fluorescence microscope using the 100×/1.45 numerical aperture (NA) objective. TIRF illumination was set up and aligned according to the manufacturer's instructions, as previously described (72). Confocal microscopy was performed on a Zeiss LSM 700 system (Carl Zeiss).

Chemokinesis assay

CHO-ICAM-1 cells (ATCC) were plated on fibronectin-coated, glass-bottom μ-dishes (ibidi) and cultured overnight until confluent. siRNA targeting SHP-1 or SHP-2 (Dharmacon ON-TARGET SMARTpool) was introduced into primary human T cells by nucleofection (Lonza). Cells were labeled with carboxyfluorescein diacetate succinimidyl ester and plated onto the CHO-ICAM-1 monolayers. Cells were allowed to settle for 3 min before the addition of the anti-CD3 antibody (1 μg/ml). Immediately after stimulation, the cells were live-imaged and a series of 30 images were captured over a period of 10 min with an inverted Zeiss 700 laser scanning confocal microscope (Carl Zeiss MicroImaging). Cell movement was analyzed by Volocity software (version 6.2.1).

Rap1 activation assay

Activated Rap1 was detected with a GST pull-down assay, as previously described (5). Jurkat cells were stimulated with anti-CD3 antibody for 2 min before being lysed. Cell lysates were incubated with GST-RBD-RalGDS coupled to glutathione beads to pull down activated Rap1. The pull-down lysates were then separated by tris-glycine poly-acrylamide gel electrophoresis (PAGE) and transferred to nitrocellulose filters. The filters were then blocked and incubated with the anti-Rap1 antibody at 4°C overnight. Immunoreactive bands were visualized with the Odyssey Imaging System (LI-COR Biosciences).

Pull-downs and Western blotting analysis

Cell lysates were mixed with anti-GFP monoclonal antibody coupled to agarose beads (MBL) to enrich GFP-tagged proteins according to the manufacturer's protocols. Pull-down lysates were separated by tris-glycine PAGE, transferred to nitrocellulose filters, and visualized as previously described (18).

FRET analysis

Cells were transfected with the PICCHUx vector, which was constructed to include cDNA encoding the human CrkII protein with YFP and CFP on both ends and an N-terminal CAAX motif (37). Three images acquired for each set of measurements were as follows: YFP excitation/YFP emission image (YFP channel), CFP excitation/CFP emission image (CFP channel), and CFP excitation/YFP emission image (FRET channel). Single-labeled (CFP or YFP) cells were used to calculate the non-FRET fluorescence bleed-through into

the FRET channel produced by the fluorophores, and the non-FRET fluorescent intensity values were subtracted from the apparent FRET intensities obtained from the double-labeled cells under the same conditions. A set of reference images was acquired from single-labeled CFP- or YFP-expressing cells for each set of acquisition parameters, and a calibration curve was derived to enable elimination of the non-FRET components from the FRET channel. The FRET efficiency was calculated on a pixel-by-pixel basis with ImageJ software version 1.48v (National Institutes of Health; http://imagej.nih.gov/ij).

Flow cytometry

Jurkat cells expressing GFP-CrkII, GFP-CrkII (Y221D), or GFP-CrkII (Y221A) were stimulated with immobilized anti-CD3 antibody and recombinant ICAM-1 for 24 hours, washed, and then incubated with PE-conjugated anti-CD69 antibody to determine the cell surface abundance of CD69 with a FACSCalibur flow cytometer.

Enzyme-linked immunosorbent assay

To determine the concentration of IL-2 secreted by cells in response to stimulation, a human IL-2 ELISA kit (BioLegend) was used according to the manufacturer's protocols. Cells were stimulated with immobilized anti-CD3 antibody and recombinant ICAM-1 for 48 hours before the cell culture medium was collected (73).

Knockdown of SHP-1 and SHP-2

Jurkat cells were infected with lentiviruses encoding shRNA specific for *SHP-1* (NM_002831.5–1391s21c1) or *SHP-2* (NM_002834.3–1570s1c1) or with a scrambled shRNA (SHC016) (multiplicity of infection of 2.5) (Mission; Sigma). Cell clones resistant to puromycin (2 μg/ml) were selected after 72 hours. Protein amounts were determined by Western blotting. For primary human T cells, siRNAs (Dharmacon SMARTpool) were introduced by nucleofection, and experiments were performed 48 hours later.

Static adhesion assay

The analysis of T cell adhesion was performed as previously described (45). Cells expressing GFP-tagged constructs were stimulated with anti-CD3 antibody before being plated on optical bottom 96-well plates (Corning) precoated with ICAM-1. Cells were incubated for 15 min to allow the cells to settle, which was followed by the removal of nonadherent cells by serial washes. The percentage of adherent cells was determined with a fluorescent plate reader (Synergy HT, BioTek).

Statistical analysis

Prism software (version 6) was used for *t* tests and ANOVA analysis.

Supplementary Material

Refer to Web version on PubMed Central for supplementary material.

Acknowledgments:

We thank M. Philips [New York University (NYU)] for helpful discussions, D. Depoil (NYU) and M. Cammer (NYU) for their assistance with the TIRF microscope, A. Pelzek (NYU) for proofreading and editing comments, N. Cohen (Columbia University) for assistance with statistical analysis, P. Stork (Vollum Institute) for providing the C3G-GFP plasmid, K. Yamada (NIH) for providing the GFP-CrkII plasmid, L. Chin (Harvard Medical School) for the Flag-CasL-HA plasmid, M. Matsuda (Osaka University) for offering the PICCHUx vector, and B. Neel (NYU) for the SHP-1-MSCV-IRES-GFP plasmid.

Funding:

This work was supported by the NIH [grants AI043542 (to M.L.D.) and R01AI125640 (to A.M.)], the Wellcome Trust [100262Z/12/Z (to M.L.D.)], the Irma T. Hirschl Trust (to A.M.), the Colton Family (to A.M.), and the Rheumatology Research Foundation (to A.M.).

REFERENCES AND NOTES

1. Smith-Garvin JE, Koretzky GA, Jordan MS, T cell activation. Annu. Rev. Immunol. 27, 591–619 (2009). [PubMed: 19132916]
2. Brownlie RJ, Zamoyska R, T cell receptor signalling networks: Branched, diversified and bounded. Nat. Rev. Immunol. 13, 257–269 (2013). [PubMed: 23524462]
3. Tapia M, Mor A, Lymphocyte adhesion and autoimmunity. Bull. Hosp. Jt. Dis. 72, 148–153 (2014).
4. Mor A, Dustin ML, Philips MR, Small GTPases and LFA-1 reciprocally modulate adhesion and signaling. Immunol. Rev. 218, 114–125 (2007). [PubMed: 17624948]
5. Azoulay-Alfaguter I, Strazza M, Pedoeem A, Mor A, The coreceptor programmed death 1 inhibits T-cell adhesion by regulating Rap1. J. Allergy Clin. Immunol. 135, 564–567.e1 (2015). [PubMed: 25240786]
6. Strazza M, Azoulay-Alfaguter I, Dun B, Baquero-Buitrago J, Mor A, CD28 inhibits T cell adhesion by recruiting CAPRI to the plasma membrane. J. Immunol. 194, 2871–2877 (2015). [PubMed: 25637021]
7. Dustin ML, Springer TA, Lymphocyte function-associated antigen-1 (LFA-1) interaction with intercellular adhesion molecule-1 (ICAM-1) is one of at least three mechanisms for lymphocyte adhesion to cultured endothelial cells. J. Cell Biol. 107, 321–331 (1988). [PubMed: 3134364]
8. Katagiri K, Hattori M, Minato N, Kinashi T, Rap1 functions as a key regulator of T-cell and antigen-presenting cell interactions and modulates T-cell responses. Mol. Cell. Biol. 22, 1001–1015 (2002). [PubMed: 11809793]
9. Comrie WA, Babich A, Burkhardt JK, F-actin flow drives affinity maturation and spatial organization of LFA-1 at the immunological synapse. J. Cell Biol. 208, 475–491 (2015). [PubMed: 25666810]
10. Kooistra MRH, Dubé N, Bos JL, Rap1: A key regulator in cell-cell junction formation. J. Cell Sci. 120, 17–22 (2007). [PubMed: 17182900]
11. Manevich-Mendelson E, Feigelson SW, Pasvolsky R, Aker M, Grabovsky V, Shulman Z, Kilic SS, Rosenthal-Allieri MA, Ben-Dor S, Mory A, Bernard A, Moser M, Etzioni A, Alon R, Loss of Kindlin-3 in LAD-III eliminates LFA-1 but not VLA-4 adhesiveness developed under shear flow conditions. Blood 114, 2344–2353 (2009). [PubMed: 19617577]
12. Kinashi T, Aker M, Sokolovsky-Eisenberg M, Grabovsky V, Tanaka C, Shamri R, Feigelson S, Etzioni A, Alon R, LAD-III, a leukocyte adhesion deficiency syndrome associated with defective Rap1 activation and impaired stabilization of integrin bonds. Blood 103, 1033–1036 (2004). [PubMed: 14551137]
13. Moser M, Nieswandt B, Ussar S, Pozgajova M, Fässler R, Kindlin-3 is essential for integrin activation and platelet aggregation. Nat. Med. 14, 325–330 (2008). [PubMed: 18278053]
14. Katagiri K, Maeda A, Shimonaka M, Kinashi T, RAPL, a Rap1-binding molecule that mediates Rap1-induced adhesion through spatial regulation of LFA-1. Nat. Immunol. 4, 741–748 (2003). [PubMed: 12845325]
15. Boettner B, Van Aelst L, Control of cell adhesion dynamics by Rap1 signaling. Curr. Opin. Cell Biol. 21, 684–693 (2009). [PubMed: 19615876]

16. Radha V, Mitra A, Dayma K, Sasikumar K, Signalling to actin: Role of C3G, a multitasking guanine-nucleotide-exchange factor. Biosci. Rep. 31, 231–244 (2011). [PubMed: 21366540]
17. Zwartkruis FJT, Bos JL, Ras and Rap1: Two highly related small GTPases with distinct function. Exp. Cell Res. 253, 157–165 (1999). [PubMed: 10579920]
18. Mor A, Wynne JP, Ahearn IM, Dustin ML, Du G, Philips MR, Phospholipase D1 regulates lymphocyte adhesion via upregulation of Rap1 at the plasma membrane. Mol. Cell. Biol. 29, 3297–3306 (2009). [PubMed: 19332557]
19. Gelkop S, Gish GD, Babichev Y, Pawson T, Isakov N, T cell activation-induced CrkII binding to the Zap70 protein tyrosine kinase is mediated by Lck-dependent phosphorylation of Zap70 tyrosine 315. J. Immunol. 175, 8123–8132 (2005). [PubMed: 16339550]
20. Nath PR, Dong G, Braiman A, Isakov N, Immunophilins control T lymphocyte adhesion and migration by regulating CrkII binding to C3G. J. Immunol. 193, 3966–3977 (2014). [PubMed: 25225668]
21. Braiman A, Isakov N, The role of Crk adaptor proteins in T-cell adhesion and migration. Front. Immunol. 6, 509 (2015). [PubMed: 26500649]
22. Huang Y, Clarke F, Karimi M, Roy NH, Williamson EK, Okumura M, Mochizuki K, Chen EJH, Park T-J, Debes GF, Zhang Y, Curran T, Kambayashi T, Burkhardt JK, CRK proteins selectively regulate T cell migration into inflamed tissues. J. Clin. Invest. 125, 1019–1032 (2015). [PubMed: 25621495]
23. Bromley SK, Burack WR, Johnson KG, Somersalo K, Sims TN, Sumen C, Davis MM, Shaw AS, Allen PM, Dustin ML, The immunological synapse. Annu. Rev. Immunol. 19, 375–396 (2001). [PubMed: 11244041]
24. Dustin ML, The immunological synapse. Cancer Immunol. Res. 2, 1023–1033 (2014). [PubMed: 25367977]
25. Bivona TG, Wiener HH, Ahearn IM, Silletti J, Chiu VK, Philips MR, Rap1 up-regulation and activation on plasma membrane regulates T cell adhesion. J. Cell Biol. 164, 461–470 (2004). [PubMed: 14757755]
26. Côte M, Fos C, Canonigo-Balancio AJ, Ley K, Bécart S, Altman A, SLAT promotes TCR-mediated, Rap1-dependent LFA-1 activation and adhesion through interaction of its PH domain with Rap1. J. Cell Sci. 128, 4341–4352 (2015). [PubMed: 26483383]
27. Wynne JP, Wu J, Su W, Mor A, Patsoukis N, Boussiotis VA, Hubbard SR, Philips MR, Rap1-interacting adaptor molecule (RIAM) associates with the plasma membrane via a proximity detector. J. Cell Biol. 199, 317–330 (2012). [PubMed: 23045549]
28. Seabra MC, Membrane association and targeting of prenylated Ras-like GTPases. Cell. Signal. 10, 167–172 (1998). [PubMed: 9607139]
29. Williams CL, The polybasic region of Ras and Rho family small GTPases: A regulator of protein interactions and membrane association and a site of nuclear localization signal sequences. Cell. Signal. 15, 1071–1080 (2003). [PubMed: 14575862]
30. Azoulay-Alfaguter I, Strazza M, Mor A, Chaperone-mediated specificity in Ras and Rap signaling. Crit. Rev. Biochem. Mol. Biol. 50, 194–202 (2015). [PubMed: 25488471]
31. Gorman JA, Babich A, Dick CJ, Schoon RA, Koenig A, Gomez TS, Burkhardt JK, Billadeau DD, The cytoskeletal adaptor protein IQGAP1 regulates TCR-mediated signaling and filamentous actin dynamics. J. Immunol. 188, 6135–6144 (2012). [PubMed: 22573807]
32. Yamashita S, Mochizuki N, Ohba Y, Tobiume M, Okada Y, Sawa H, Nagashima K, Matsuda M, CalDAG-GEFIII activation of Ras, R-ras, and Rap1. J. Biol. Chem. 275, 25488–25493 (2000). [PubMed: 10835426]
33. Sawasdikosol S, Ravichandran KS, Lee KK, Chang J-H, Burakoff SJ, Crk interacts with tyrosine-phosphorylated p116 upon T cell activation. J. Biol. Chem. 270, 2893–2896 (1995). [PubMed: 7531694]
34. Reedquist KA, Fukazawa T, Panchamoorthy G, Langdon WY, Shoelson SE, Druker BJ, Band H, Stimulation through the T cell receptor induces Cbl association with Crk proteins and the guanine nucleotide exchange protein C3G. J. Biol. Chem. 271, 8435–8442 (1996). [PubMed: 8626543]
35. Liu D, The adaptor protein Crk in immune response. Immunol. Cell Biol. 92, 80–89 (2014). [PubMed: 24165979]

36. Huyer G, Liu S, Kelly J, Moffat J, Payette P, Kennedy B, Tsaprailis G, Gresser MJ, Ramachandran C, Mechanism of inhibition of protein-tyrosine phosphatases by vanadate and pervanadate. J. Biol. Chem. 272, 843–851 (1997). [PubMed: 8995372]
37. Kurokawa K, Mochizuki N, Ohba Y, Mizuno H, Miyawaki A, Matsuda M, A pair of fluorescent resonance energy transfer-based probes for tyrosine phosphorylation of the CrkII adaptor protein in vivo. J. Biol. Chem. 276, 31305–31310 (2001). [PubMed: 11406630]
38. Mor A, Campi G, Du G, Zheng Y, Foster DA, Dustin ML, Philips MR, The lymphocyte function-associated antigen-1 receptor costimulates plasma membrane Ras via phospholipase D2. Nat. Cell Biol. 9, 713–719 (2007). [PubMed: 17486117]
39. Sojka DK, Bruniquel D, Schwartz RH, Singh NJ, IL-2 secretion by $CD4^+$ T cells in vivo is rapid, transient, and influenced by TCR-specific competition. J. Immunol. 172, 6136–6143 (2004). [PubMed: 15128800]
40. Nolz JC, Nacusi LP, Segovis CM, Medeiros RB, Mitchell JS, Shimizu Y, Billadeau DD, The WAVE2 complex regulates T cell receptor signaling to integrins via Abl- and CrkL–C3G-mediated activation of Rap1. J. Cell Biol. 182, 1231–1244 (2008). [PubMed: 18809728]
41. Chen L, Sung S-S, Yip MLR, Lawrence HR, Ren Y, Guida WC, Sebti SM, Lawrence NJ, Wu J, Discovery of a novel shp2 protein tyrosine phosphatase inhibitor. Mol. Pharmacol. 70, 562–570 (2006). [PubMed: 16717135]
42. Li Y-M, Casida JE, Cantharidin-binding protein: Identification as protein phosphatase 2A. Proc. Natl. Acad. Sci. U.S.A. 89, 11867–11870 (1992). [PubMed: 1334551]
43. Stanford SM, Rapini N, Bottini N, Regulation of TCR signalling by tyrosine phosphatases: From immune homeostasis to autoimmunity. Immunology 137, 1–19 (2012).
44. Chong ZZ, Maiese K, The Src homology 2 domain tyrosine phosphatases SHP-1 and SHP-2: Diversified control of cell growth, inflammation, and injury. Histol. Histopathol. 22, 1251–1267 (2007). [PubMed: 17647198]
45. Strazza M, Azoulay-Alfaguter I, Pedoeem A, Mor A, Static adhesion assay for the study of integrin activation in T lymphocytes. J. Vis. Exp. 2014, e51646 (2014).
46. Schneider H, Downey J, Smith A, Zinselmeyer BH, Rush C, Brewer JM, Wei B, Hogg N, Garside P, Rudd CE, Reversal of the TCR stop signal by CTLA-4. Science 313, 1972–1975 (2006). [PubMed: 16931720]
47. Gotoh T, Hattori S, Nakamura S, Kitayama H, Noda M, Takai Y, Kaibuchi K, Matsui H, Hatase O, Takahashi H, Kurata T, Matsuda M, Identification of Rap1 as a target for the Crk SH3 domain-binding guanine nucleotide-releasing factor C3G. Mol. Cell. Biol. 15, 6746–6753 (1995). [PubMed: 8524240]
48. Birge RB, Kalodimos C, Inagaki F, Tanaka S, Crk and CrkL adaptor proteins: Networks for physiological and pathological signaling. Cell Commun. Signal. 7, 13 (2009). [PubMed: 19426560]
49. Ohashi Y, Tachibana K, Kamiguchi K, Fujita H, Morimoto C, T cell receptor-mediated tyrosine phosphorylation of Cas-L, a 105-kDa Crk-associated substrate-related protein, and its association of Crk and C3G. J. Biol. Chem. 273, 6446–6451 (1998). [PubMed: 9497377]
50. Campi G, Varma R, Dustin ML, Actin and agonist MHC–peptide complex–dependent T cell receptor microclusters as scaffolds for signaling. J. Exp. Med. 202, 1031–1036 (2005). [PubMed: 16216891]
51. Billadeau DD, T cell activation at the immunological synapse: Vesicles emerge for LATer signaling. Sci. Signal. 3, pe16 (2010).
52. Purbhoo MA, Liu H, Oddos S, Owen DM, Neil MAA, Pageon SV, French PMW, Rudd CE, Davis DM, Dynamics of subsynaptic vesicles and surface microclusters at the immunological synapse. Sci. Signal. 3, ra36 (2010).
53. Mor A, Philips MR, Compartmentalized Ras/MAPK signaling. Annu. Rev. Immunol. 24, 771–800 (2006). [PubMed: 16551266]
54. Sarkar P, Reichman C, Saleh T, Birge RB, Kalodimos CG, Proline *cis-trans* isomerization controls autoinhibition of a signaling protein. Mol. Cell 25, 413–426 (2007). [PubMed: 17289588]
55. Sarkar P, Saleh T, Tzeng S-R, Birge RB, Kalodimos CG, Structural basis for regulation of the Crk signaling protein by a proline switch. Nat. Chem. Biol. 7, 51–57 (2011). [PubMed: 21131971]

56. Nath PR, Isakov N, Insights into peptidyl-prolyl *cis-trans* isomerase structure and function in immunocytes. Immunol. Lett. 163, 120–131 (2015). [PubMed: 25445495]
57. Nath PR, Dong G, Braiman A, Isakov N, In vivo regulation of human CrkII by cyclophilin A and FK506-binding protein. Biochem. Biophys. Res. Commun. 470, 411–416 (2016). [PubMed: 26792730]
58. Kumari S, Vardhana S, Cammer M, Curado S, Santos L, Sheetz MP, Dustin ML, T lymphocyte myosin IIA is required for maturation of the immunological synapse. Front. Immunol. 3, 230 (2012). [PubMed: 22912631]
59. Choudhuri K, Llodrá J, Roth EW, Tsai J, Gordo S, Wucherpfennig KW, Kam LC, Stokes DL, Dustin ML, Polarized release of T-cell-receptor-enriched microvesicles at the immunological synapse. Nature 507, 118–123 (2014). [PubMed: 24487619]
60. Yarden Y, Ullrich A, Growth factor receptor tyrosine kinases. Annu. Rev. Biochem. 57, 443–478 (1988). [PubMed: 3052279]
61. Hunter T, Protein modification: Phosphorylation on tyrosine residues. Curr. Opin. Cell Biol. 1, 1168–1181 (1989). [PubMed: 2561455]
62. Kwon J, Qu C-K, Maeng J-S, Falahati R, Lee C, Williams MS, Receptor-stimulated oxidation of SHP-2 promotes T-cell adhesion through SLP-76–ADAP. EMBO J. 24, 2331–2341 (2005). [PubMed: 15933714]
63. Yu Y, Smoligovets AA, Groves JT, Modulation of T cell signaling by the actin cytoskeleton. J. Cell Sci. 126, 1049–1058 (2013). [PubMed: 23620508]
64. Dustin ML, Groves JT, Receptor signaling clusters in the immune synapse. Annu. Rev. Biophys. 41, 543–556 (2012). [PubMed: 22404679]
65. Dehring DAK, Clarke F, Ricart BG, Huang Y, Gomez TS, Williamson EK, Hammer DA, Billadeau DD, Argon Y, Burkhardt JK, Hematopoietic lineage cell-specific protein 1 functions in concert with the Wiskott-Aldrich syndrome protein to promote podosome array organization and chemotaxis in dendritic cells. J. Immunol. 186, 4805–4818 (2011). [PubMed: 21398607]
66. Sasahara Y, Rachid R, Byrne MJ, de la Fuente MA, Abraham RT, Ramesh N, Geha RS, Mechanism of recruitment of WASP to the immunological synapse and of its activation following TCR ligation. Mol. Cell 10, 1269–1281 (2002). [PubMed: 12504004]
67. Raab M, Smith X, Matthess Y, Strebhardt K, Rudd CE, SKAP1 protein PH domain determines RapL membrane localization and Rap1 protein complex formation for T cell receptor (TCR) activation of LFA-1. J. Biol. Chem. 286, 29663–29670 (2011). [PubMed: 21669874]
68. Raab M, Wang H, Lu Y, Smith X, Wu Z, Strebhardt K, Ladbury JE, Rudd CE, T cell receptor "inside-out" pathway via signaling module SKAP1-RapL regulates T cell motility and interactions in lymph nodes. Immunity 32, 541–556 (2010). [PubMed: 20346707]
69. Su W, Wynne J, Pinheiro EM, Strazza M, Mor A, Montenont E, Berger J, Paul DS, Bergmeier W, Gertler FB, Philips MR, Rap1 and its effector RIAM are required for lymphocyte trafficking. Blood 126, 2695–2703 (2015). [PubMed: 26324702]
70. Choy E, Chiu VK, Silletti J, Feoktistov M, Morimoto T, Michaelson D, Ivanov IE, Philips MR, Endomembrane trafficking of ras: The CAAX motif targets proteins to the ER and Golgi. Cell 98, 69–80 (1999). [PubMed: 10412982]
71. Kloog Y, Mor A, Cytotoxic-T-lymphocyte antigen 4 receptor signaling for lymphocyte adhesion is mediated by C3G and Rap1. Mol. Cell. Biol. 34, 978–988 (2014). [PubMed: 24396067]
72. Varma R, Campi G, Yokosuka T, Saito T, Dustin ML, T cell receptor-proximal signals are sustained in peripheral microclusters and terminated in the central supramolecular activation cluster. Immunity 25, 117–127 (2006). [PubMed: 16860761]
73. Zanin-Zhorov A, Weiss JM, Nyuydzefe MS, Chen W, Scher JU, Mo R, Depoil D, Rao N, Liu B, Wei J, Lucas S, Koslow M, Roche M, Schueller O, Weiss S, Poyurovsky MV, Tonra J, Hippen KL, Dustin ML, Blazar BR, Liu C.-j., Waksal SD, Selective oral ROCK2 inhibitor down-regulates IL-21 and IL-17 secretion in human T cells via STAT3-dependent mechanism. Proc. Natl. Acad. Sci. U.S.A. 111, 16814–16819 (2014). [PubMed: 25385601]

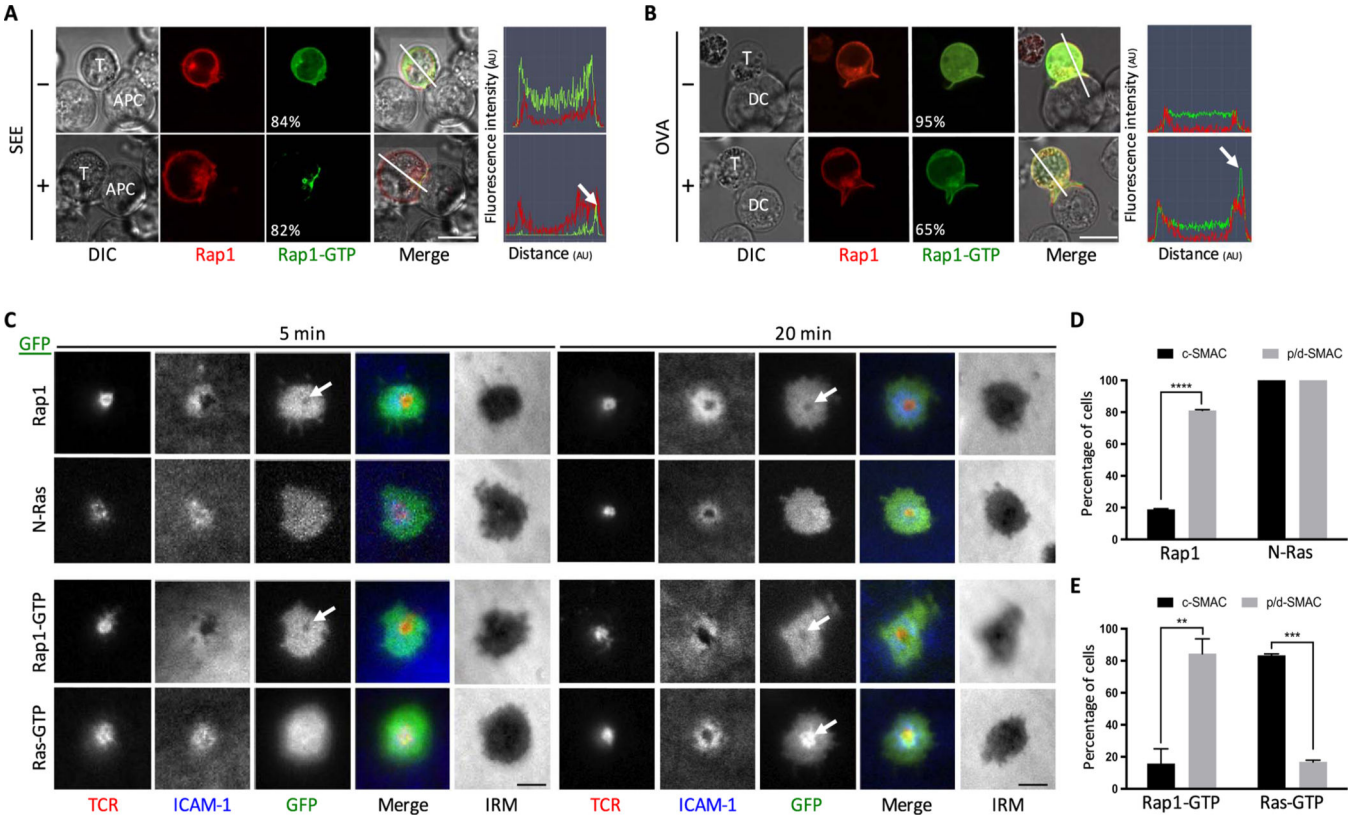

Fig. 1. Activated Rap1 is recruited to the immunological synapse.

(**A**) Jurkat cells were cotransfected with plasmids encoding GFP-RalGDS-RBD (the probe for activated Rap1) and Cherry-Rap1, cocultured with Raji cells (APCs) preloaded with SEE (1.5 μg/ml), and subjected to live imaging. Images are representative of at least 50 cells from each of three independent experiments. DIC, differential interference contrast; AU, arbitrary units. Line profile analysis is quantified as fluorescent intensity units over distance. (**B**) OT-II T cells were cotransfected with plasmids encoding GFP-RalGDS-RBD and Cherry-Rap1, cocultured with DCs pulsed with OVA peptide (100 μg/ml), and subjected to live imaging. Line profile analysis is quantified as fluorescent intensity units over distance. (**C** to **E**) Primary human T cells were transfected with plasmids encoding GFP-tagged Rap1, N-Ras, RalGDS-RBD, or Raf1-RBD (the probe for activated Ras), as indicated. The cells were then introduced onto SLBs containing anti-CD3 antibody (5 μg/ml) labeled with Alexa Fluor 568 (to label the TCR) and ICAM-1 (250 molecules/mm^2) tagged with Alexa Fluor 405. Live cells were imaged by TIRF microscopy at the indicated times. (D and E) Quantification of the distribution of the GFP-tagged proteins within the indicated compartments of the immunological synapse at the 20-min time point. Data are means ± SEM of at least 50 cells from each of three experiments. $^{**}P < 0.01$, $^{***}P < 0.001$, $^{****}P < 0.0001$ by unpaired *t* test. Scale bars, 10 μm. IRM, interference reflection microscopy.

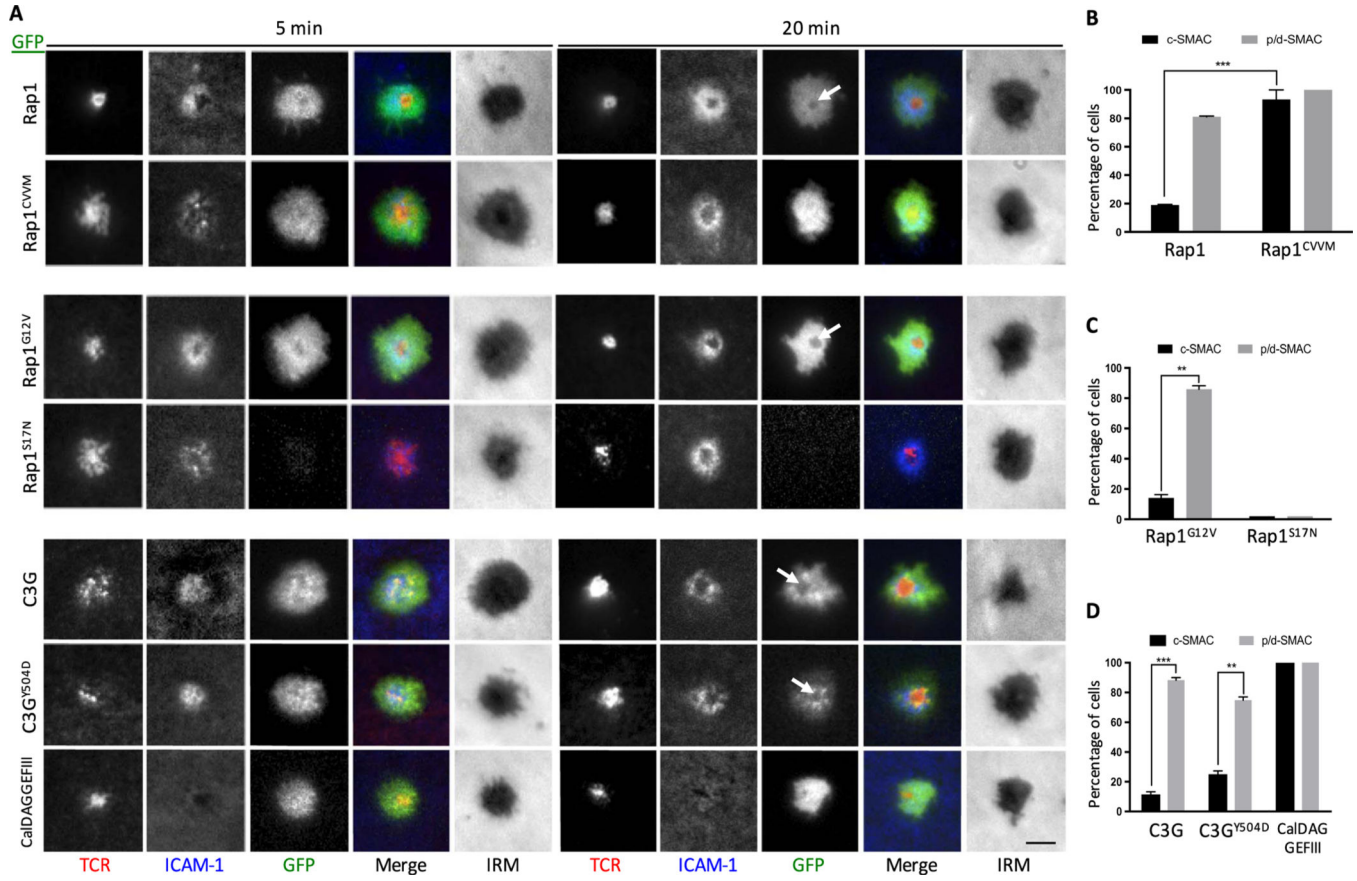

Fig. 2. Analysis of the factors regulating Rap1 localization in the immunological synapse.

(**A**) Primary human T cells expressing GFP-tagged Rap1 (wild type), GFP-Rap1^{CVVM} (Rap1 with N-Ras tail), GFP-Rap1^{G12V} (GTP-loaded Rap1), GFP-Rap1^{S17N} (GDP-loaded Rap1), GFP-C3G, GFP-C3G^{Y504D} (phosphomimetic), or GFP-CalDAG-GEFIII were introduced onto SLBs containing anti-CD3 antibody (5 μg/ml) labeled with Alexa Fluor 568 and ICAM-1 (250 molecules/mm^2) tagged with Alexa Fluor 405 and subjected to live imaging by TIRF microscopy at the indicated times. (**B** to **D**) Quantification of the distribution of the indicated GFP-tagged proteins within the different compartments of the immunological synapse at the 20-min time point. Data are means ± SEM of at least 50 cells from more than three experiments. $^{**}P < 0.01$, $^{***}P < 0.001$, by two-way analysis of variance (ANOVA) and unpaired *t* tests. Scale bar, 10 μm.

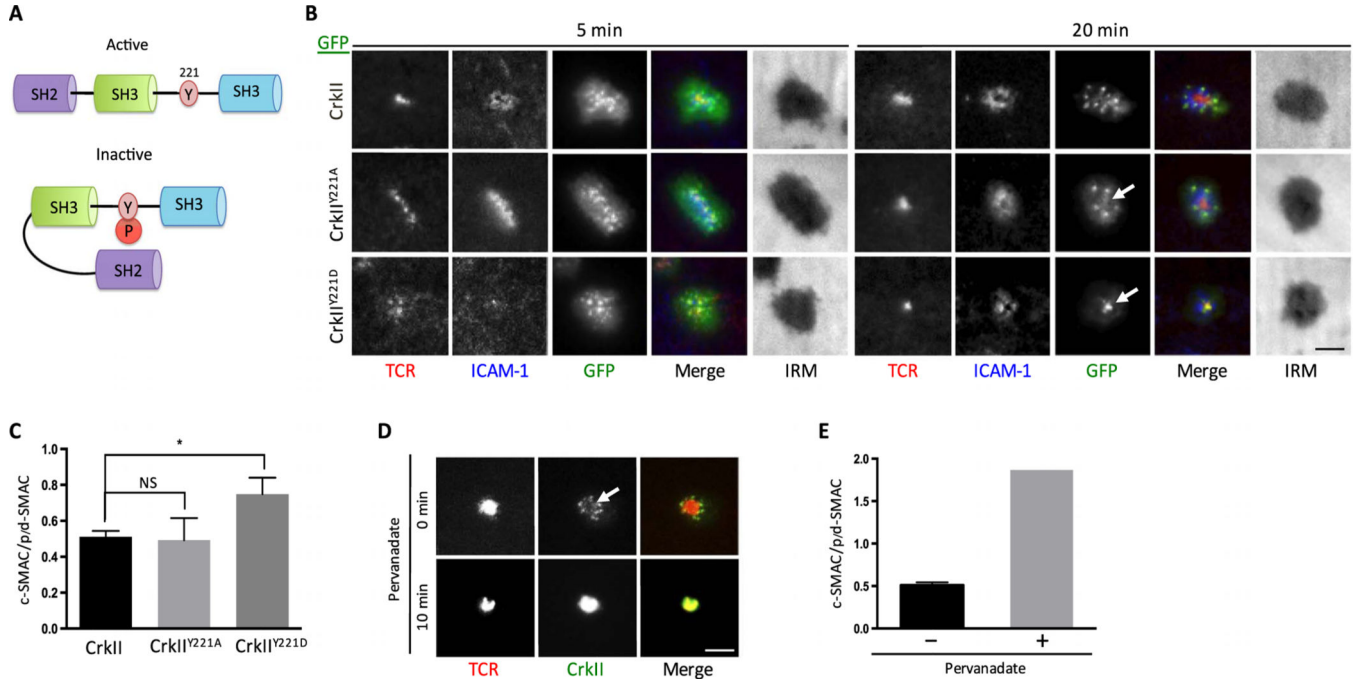

Fig. 3. CrkII phosphorylation is required for its proper localization in the immunological synapse.

(**A**) Domain structures of active (dephosphorylated) and inactive (phosphorylated) CrkII. (**B**) Primary human T cells were transfected with plasmids encoding GFP-tagged wild-type CrkII, phosphodeficient CrkII (Y221A), or phosphomimetic CrkII (Y221D). The cells were injected onto SLBs containing fluorescently labeled anti-CD3 antibody (5 μg/ml) and ICAM-1 (250 molecules/mm^2) and subjected to live imaging at different time points. (**C**) Quantification of the relative distribution of the different versions of CrkII in the immunological synapse. (**D**) Primary human T cells expressing GFP-CrkII were plated on SLBs containing fluorescently labeled anti-CD3 antibody (5 μg/ml) and ICAM-1 (250 molecules/mm^2), treated with 50 μM pervanadate, and subjected to live imaging. (**E**) Quantification of the relative distribution or CrkII before and after treatment with pervanadate within the different compartments of the immunological synapse. Data are means ± SEM of at least 25 cells from each of three experiments. *$P < 0.05$, by unpaired t tests. NS, not significant. Scale bar, 10 μm.

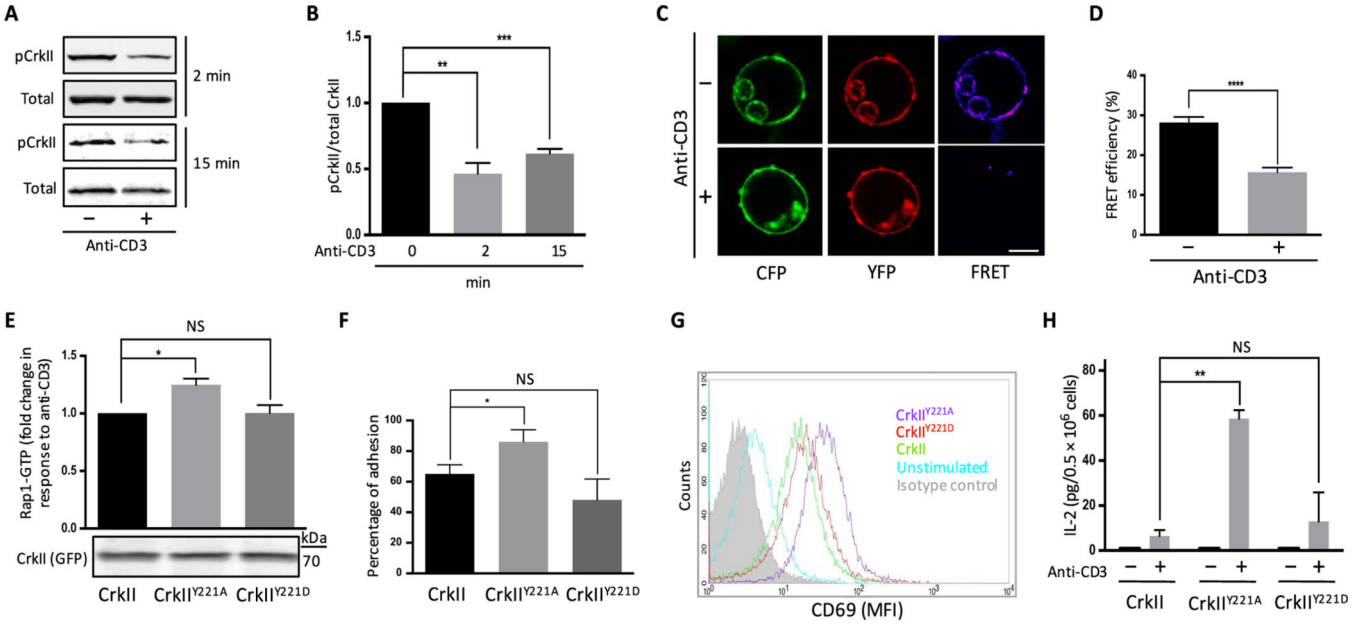

Fig. 4. CrkII dephosphorylation leads to T cell activation.

(**A**) Jurkat cells were stimulated with anti-CD3 antibody (5 μg/ml) for 2 to 15 min, lysed, and then analyzed by Western blotting with antibodies against phosphorylated and total CrkII proteins. (**B**) Quantification of the ratio between phosphorylated CrkII and total CrkII after stimulation with anti-CD3 antibody (5 μg/ml). (**C**) Jurkat cells expressing the PICCHUx construct (YFP-CrkII-CFP-CAAX) were treated with anti-CD3 antibody (5 μg/ml) and fixed with 2% paraformaldehyde. FRET emission was then recorded (excitation at 433 nm; emission at 530 nm). (**D**) Quantification of FRET efficiency in the indicated cells. (**E**) Jurkat cells expressing GFP-CrkII (wild type), GFP-CrkII^{Y221A}, or GFP-CrkII^{Y221D} were stimulated with anti-CD3 antibody (5 μg/ml), and the amounts of activated Rap1 were measured by glutathione *S*-transferase (GST) pull-down assay. (**F**) Jurkat cells expressing GFP-CrkII (wild type), GFP-CrkII^{Y221A}, or GFP-CrkII^{Y221D} were stimulated with anti-CD3 antibody (5 μg/ml), and the percentages of cells that exhibited adhesion to ICAM-1–coated wells were measured. (**G**) Jurkat cells expressing GFP-CrkII, GFP-CrkII^{Y221A}, or GFP-CrkII^{Y221D} were stimulated with anti-CD3 antibody (1 μg/ml), plated overnight on wells coated with ICAM-1 (2 μg/ml), and then subjected to flow cytometry analysis of the relative amounts of cell surface CD69. MFI, mean fluorescence intensity. (**H**) Jurkat cells expressing GFP-CrkII, GFP-CrkII^{Y221A}, or GFP-CrkII^{Y221D} were stimulated with anti-CD3 antibody (1 μg/ml) and plated on wells coated with ICAM-1 (2 μg/ml). Forty-eight hours later, the amounts of IL-2 in the cell culture medium were measured. Data in all panels are means ± SEM of three experiments. *$P < 0.05$, **$P < 0.01$, ***$P < 0.001$, ****$P < 0.0001$, by unpaired *t* tests and two-way ANOVA. Scale bar, 10 μm.

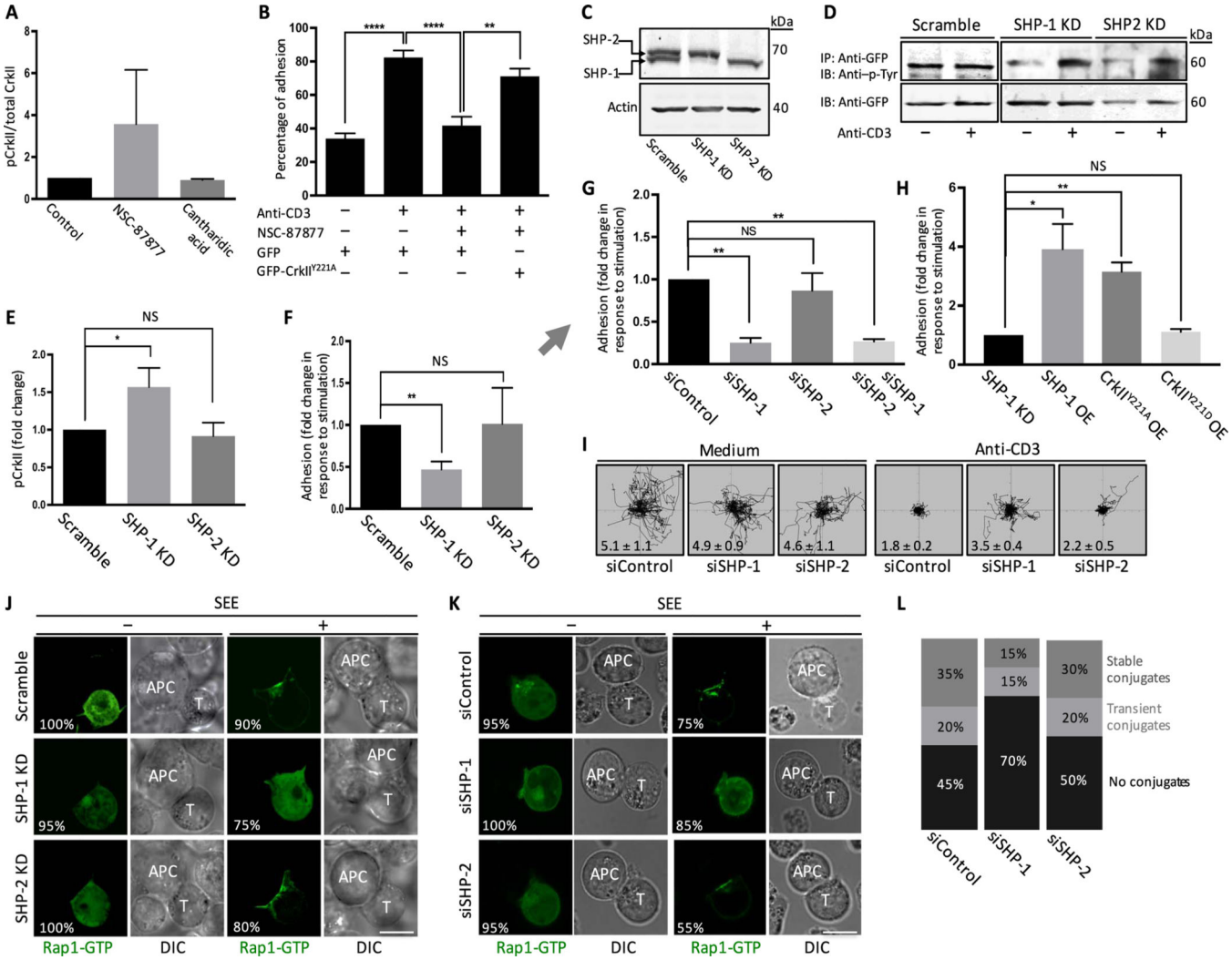

Fig. 5. SHP-1 dephosphorylates CrkII downstream of TCR activation.

(**A**) Jurkat cells expressing GFP-CrkII were pretreated with SHP-1/2 inhibitor (20 mM NSC-87877) or PP2A inhibitor (400 mM cantharidic acid) for 30 min, stimulated with anti-CD3 antibody (5 μg/ml) for 2 min, lysed, and subjected to Western blotting analysis of the extent of CrkII phosphorylation. The ratios of the relative amount of phosphorylated CrkII to that of total CrkII were determined. Data are means ± SEM of three experiments. (**B**) Jurkat cells expressing GFP or GFP-CrkII^{Y221A} were pretreated with 20 nM NSC-87877 for 30 min before being stimulated with anti-CD3 antibody (1 μg/ml) and plated on ICAM-1–coated wells. The percentages of adherent cells after 15 min were measured. (**C**) Jurkat cells were infected with lentiviruses encoding scrambled shRNA or shRNAs targeting *SHP-1* or *SHP-2*. The relative amounts of SHP-1 and SHP-2 were analyzed by Western blotting. (**D**) Jurkat cells expressing GFP-CrkII and the indicated shRNAs were treated with anti-CD3 antibody (5 μg/ml) for 5 min. Cell lysates were then subjected to immunoprecipitation (IP) with anti-GFP antibody and Western blotting (IB) analysis with anti–p-Tyr antibody. (**E**) Quantification of the indicated band intensities from three Western blotting experiments. (**F** and **G**) Jurkat cells expressing the indicated shRNAs (F) or primary human T cells

treated with control, SHP-1–specific, or SHP-2–specific siRNAs (G) were treated with anti-CD3 antibody (5 μg/ml), and the fold change in the numbers of cells that adhered to ICAM-1–coated wells was measured. (**H**) *SHP-1* was either knocked down with shRNA (SHP-1 KD) in Jurkat cells expressing GFP or rescued by overexpressing (OE) $CrkII^{Y221A}$ (GFP-$CrkII^{Y221A}$), $CrkII^{Y221D}$ (GFP-$CrkII^{Y221D}$), or an alternative SHP-1 construct (GFP-SHP-1). The cells were then treated with anti-CD3 antibody (5 μg/ml), and adhesion to ICAM-1–coated wells was measured. (**I**) Primary human T cells treated with the indicated siRNAs were stimulated with soluble anti-CD3 antibody (5 μg/ml) and assessed for motility on ICAM-1–coated plates. Between 20 and 50 cells were counted per field. (**J**) Jurkat cells expressing GFP-RalGDS-RBD and either shSHP-1 or shSHP-2 constructs were cocultured with Raji cells preloaded with SEE (1.5 μg/ml) and subjected to live imaging. (**K**) Primary human T cells expressing GFP-RalGDS-RBD and treated with the indicated siRNAs were cocultured with SEE-preloaded Raji cells and subjected to live imaging. The percentages of cells of the predominant phenotype are shown. (**L**) Primary human T cells were treated with the indicated siRNAs and cocultured with SEE-preloaded Raji cells. The percentages of cells that formed transient or stable conjugates were recorded. Data in all panels are means ± SEM of three or four independent experiments. $*P < 0.05$, $**P < 0.01$, $****P < 0.0001$, by unpaired *t* tests. Scale bars, 10 μm.

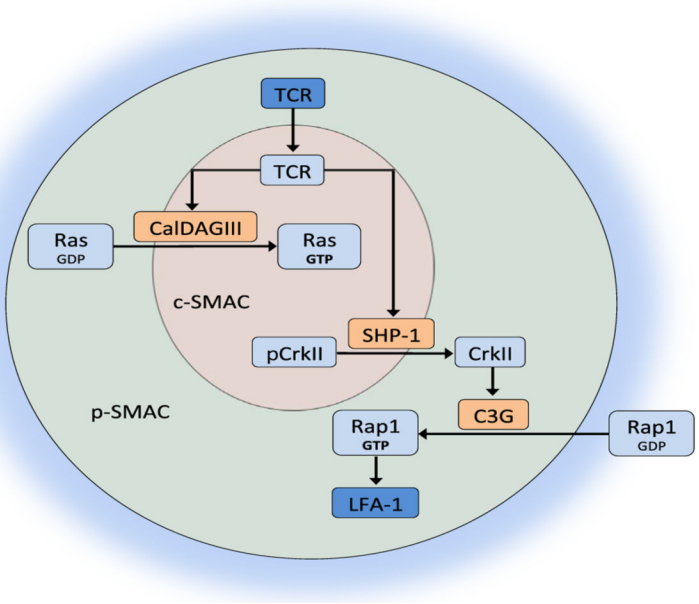

Fig. 6. Model for the localization and function of CrkII within the immunological synapse.
Stimulation of the TCR leads to the SHP-1–mediated dephosphorylation of CrkII, which then travels from the c-SMAC to the p-SMAC. Here, CrkII binds to the exchange factor C3G, which directly activates Rap1, leading to LFA-1 activation and enhanced T cell adhesion.